

# Historical review of advanced materials for electromagnetic interference (EMI) shielding: Conjugated polymers, carbon nanotubes, graphene based composites

Parveen Saini\*

CSIR-National Physical Laboratory, New Delhi 110 012, India

Received 18 June 2017; accepted 1 March 2019

Electromagnetic (EM) interference (EMI) “an off-shoot of explosive growth of electronics and telecommunications” is becoming an alarming issue for modern society. It may degrade the EM device performance or may adversely affect human health. Recently, polymer based blends and composites have emerged as powerful solution for efficient suppression of EM noises; thanks to the unique combination of electrical, thermal, dielectric, magnetic and/or mechanical properties, possessed by them. This review focuses on the basics of EMI shielding/microwave absorption, various techniques for measurement of shielding effectiveness, theoretical aspects of shielding, governing equations. In addition, different strategies and potential materials for handling of EMI have also been discussed with special reference to polymer based blends and composites especially those based on carbon nanotubes (CNTs), graphene and intrinsically conducting polymers (ICPs).

**Keywords:** Electromagnetic interference (EMI) shielding, Shielding effectiveness, Reflection loss, Absorption loss, Microwave absorption, Conductivity, Intrinsically conducting polymers (ICPs), Carbon nanotubes (CNTs), MWCNTs, SWCNTs, Graphene, Nanocomposites, Complex permittivity and permeability

## 1 Introduction

Electromagnetic interference (EMI) is an offshoot of explosive growth of electronics which may degrade the device performance and may even adversely affect the human health<sup>1-3</sup>. The arrival of nanotechnology and miniaturization of chips/devices has further aggravated the EMI issue as mutual interference among device’s components or chip elements can produce microscopic interference effects<sup>2</sup>. The most common instances of EMI from everyday life are cross-talking of our laptop screen or conference room wireless microphones with mobile-phone signals producing picture flicker or noise distortion<sup>4</sup>. Due to EMI problems; use of mobile phone is prohibited onboard or inside premises of hospitals or defence bases<sup>4-7</sup>. This necessitates the development of suitable countermeasures to suppress (or eliminate) EMI effects. Basically, there are three main mechanisms for EMI shielding viz. reflection, absorption and multiple reflection<sup>1,8,9</sup>. Among them reflection, is identified as primary EMI shielding mechanism for which the shield must contain mobile charge carriers (e.g., electrons or holes that can be provided by metallic, carbon or conducting polymer based materials). The secondary EMI shielding mechanism

is absorption for which shield should possess electric and/or magnetic dipoles (that can be provided by high permittivity or permeability materials, e.g., BaTiO<sub>3</sub> or Fe<sub>3</sub>O<sub>4</sub>) which can interact with the electric or magnetic fields in the EM radiation. The tertiary mechanism is multiple reflection, which is facilitated by high interfacial area (e.g., for porous materials)<sup>2,3,10-16</sup>. Hence, continued efforts have been made over past two decades to eliminate or suppress EMI via different strategies and variety of materials including metals, carbon based materials, conducting polymers, dielectric/magnetic materials<sup>2,6,9,11,16-41</sup>. However, despite being so much progress, still a lot to be done to realize the theoretically predicted shielding performance of a materials and to meet the other design considerations. Therefore, before selecting or designing a shielding material, basic understanding of shielding theory becomes absolutely essential.

## 2 EMI Shielding Phenomenon: Mechanisms and Mathematical Expressions

The efficiency of EM shield is expressed in terms of quantity called “Shielding Effectiveness (SE)” that can be expressed as<sup>4,8,9,11,42,43</sup>:

$$SE_T \text{ (dB)} = SE_R + SE_A + SE_M = 10 \log_{10} \left( \frac{P_T}{P_I} \right) = 20 \log_{10} \left( \frac{E_T}{E_I} \right) = 20 \log_{10} \left( \frac{H_T}{H_I} \right) \quad \dots(1)$$

\*E-mail: pksaini@nplindia.org; parveensaini580@gmail.com

where  $P_I$  ( $E_I$  or  $H_I$ ) and  $P_T$  ( $E_T$  or  $H_T$ ) are the power (electric or magnetic field intensity) of incident and transmitted EM waves respectively. In actual practice, three different phenomenon named reflection ( $SE_R$ ), absorption ( $SE_A$ ) and multiple reflections ( $SE_M$ ) contribute towards  $SE_T$  (i.e.  $SE_T = SE_R + SE_A + SE_M$ ) which can be theoretically expressed as<sup>1,2,10,43</sup>:

$$SE_R \text{ (dB)} = -10 \log_{10} \left( \frac{\sigma_T}{16\omega \epsilon_r \epsilon_o \mu_r} \right) \quad \dots(2)$$

$$SE_A \text{ (dB)} = -20 \left( \frac{t}{\delta} \right) \log_{10} e = -8.68 \left( \frac{t}{\delta} \right) = -8.68 t \sqrt{\sigma f \mu} \quad \dots(3)$$

$$SE_M \text{ (dB)} = 20 \log_{10} \left| 1 - e^{-2t/\delta} \right| = 20 \log_{10} \left( \left| 1 - 10^{-\frac{SE_A}{10}} \right| \right) \quad \dots(4)$$

where  $\sigma_T$  is the total conductivity,  $\omega$  is the angular frequency,  $\epsilon_r$  is relative permittivity,  $\mu_r$  is relative permeability referred to free space ( $\epsilon_o$ ) and  $\delta$  is skin depth (the distance required by the wave to be attenuated to  $1/e$  or 37%). The above expression shows that  $SE_R$  is a function of the ratio of conductivity ( $\sigma$ ) and permeability ( $\mu$ ) of the shield material, i.e., quantity ( $\sigma/\mu$ ) whereas  $SE_A$  is related to the product of  $\mu$  and  $\sigma$ , i.e., quantity ( $\sigma \cdot \mu$ )<sup>2,6,7,41,44</sup>. Further, it can be seen that  $SE_M$  is closely related to absorption loss ( $SE_A$ ) and can be neglected ( $SE_M \approx 0$ ) in all cases where  $SE_A$  is  $\geq 10$  dB<sup>2,14,44</sup> which is generally the case at very high frequencies ( $\sim$ GHz or high). Experimentally, shielding is measured using instruments called network analyzer<sup>9</sup> (NA) that can measure magnitude and/or phase of the incident/transmitted signals. The incident and transmitted waves in a two port vector NA (VNA), can be expressed in terms of complex scattering parameters (or S-parameters), i.e.,  $S_{11}$  (or  $S_{22}$ ) and  $S_{12}$  (or  $S_{21}$ ), respectively. The reflectance ( $R$ ) and transmittance ( $T$ ) can be expressed as:  $T = |E_T/E_I|^2 = |S_{12}|^2 = |S_{21}|^2$ ,  $R = |E_R/E_I|^2 = |S_{11}|^2 = |S_{22}|^2$ , giving absorbance ( $A$ ) as:  $A = (1-R-T)$ . The intensity of the EM wave inside the shield after primary reflection is based on quantity  $(1-R)$  so that effective absorbance  $\{A_{\text{eff}} = [(1-R-T)/(1-R)]\}$  can be defined and reflection and absorption losses can be expressed as<sup>4,10,26,43,44</sup>:

$$SE_R \text{ (dB)} = 10 \log_{10} (1 - R) \quad \dots(5)$$

$$SE_A \text{ (dB)} = 10 \log_{10} (1 - A_{\text{eff}}) = 10 \log_{10} \left[ \frac{T}{(1-R)} \right] \quad \dots(6)$$

Therefore, from the measured S-parameters, VNA automatically compute 'R' and 'T' that leads to estimation of reflection and absorption loss components of total shielding effectiveness. The electromagnetic attributes of a shield like complex permittivity [ $\epsilon^* = (\epsilon' - j\epsilon'')$ ] and permeability [ $\mu^* = (\mu' - j\mu'')$ ] can be retrieved from the experimental S-parameters [ $S_{11}$  (or  $S_{22}$ ) and  $S_{21}$  (or  $S_{12}$ )] using suitable algorithms and models viz. Nicolson-Ross-Weir (NRW), NIST iterative, New non-iterative, Short circuit line (SCL) techniques<sup>2,4,11,42,45,46</sup>. The parameter  $\epsilon'$  or  $\epsilon_r$  (real permittivity) represents the charge storage (or dielectric constant) whereas  $\epsilon''$  (imaginary permittivity) is a measure of dielectric dissipation or losses. Similarly,  $\mu'$  (or  $\epsilon_r$ ) and  $\mu''$  represent magnetic storage and losses, respectively.

### 3 Materials for EMI Shielding

It is clear from previous discussions that realization of efficient EMI shielding action requires balanced combination of electrical conductivity ( $\sigma$ ), dielectric permittivity ( $\epsilon$ ), magnetic permeability ( $\mu$ ) and morphology (e.g., porous structure) to introduce reflection, absorption and multiple reflection losses<sup>6,8,9</sup>. Metals are by far the most common materials for EMI shielding owing to their high electrical conductivity.

However, they are suffered from problems<sup>5,9,10,15,37,53,65</sup> such as high reflectivity, corrosion susceptibility, weight penalty and uneconomic processing. In this consideration, polymer based blends and composites have attracted enormous attention due to unique combination of electrical, thermal, dielectric, magnetic and/or mechanical properties useful for efficient electromagnetic shielding response. Therefore, in the recent past a large number of polymer composites have been prepared for electromagnetic applications (Table 1) using various fillers (e.g., conducting polymers, carbon nanotubes (CNTs) and graphene based materials) and polymer matrices<sup>2,4,5,8-12,14,16-18, 25-27,32,35,37,37,39,41,47-50,53-59,61-63,63-73</sup>.

#### 3.1 Carbon nanotubes (CNTs)

In the recent past, CNTs (single wall carbon nanotubes (SWCNTs) or multiwall carbon nanotubes

Table 1 – EMI shielding performance of CNTs, graphene and ICPs based composites.

Materials	Filler content	EMI SE (dB)	Band	Thickness (mm)	Reference
MWCNT/PS	7 wt%	~19	8.2-12.4 GHz	1.2	5
MWCNT/flurocarbon	12 wt%	~42-48	8.2-12.4 GHz	3.8	22
MWCNT/poly( $\epsilon$ -caprolactone)	2 wt%	~60-80	25-40 GHz	20	33
MWCNT/PP	7.5 vol%	~35	8.2-12.4 GHz	1.0	20
MWCNT/PC	5 wt %	~25	8.2-12.4 GHz	1.85	47
SWCNT/epoxy	15 wt%	~15-49	10 MHz-1.5 Ghz	1.5	48
SWCNT/epoxy	15 wt%	~20-30	8.2-12.4 GHz	2.0	22
SWCNT/PU	20 wt%	~17	8.2-12.4 GHz	2.0	12
Fe-MWCNT/epoxy	10 wt%	~32	13.2 GHz	1.0	49
MWCNT/epoxy	8 wt %	~60-90	4-26 GHz	2.0	50
MWCNT/SMP	6.7 wt %	~32-39 ~42-56 ~52-69	8-26.5 GHz 33-50 GHz 50-75 GHz	3.0	51
Fe-MWCNT/PMMA	40 wt %	~27	50MHz-13.5 GHz	0.06-0.165	52
PTT/MWCNT	10 wt%	~36-42	12.4-18.0 GHz	2.0	53
f-MWCNT/PVDF	7 wt%	~18	8.2-12.4 GHz	1.0	117
LDPE/MWCNT	10 wt%	~23	12.4-18.0 GHz	1.65	54
Graphene/PDMS	~0.8 wt%	~28-33 ~21-25	30 MHz-1.5 GHz 12.4-18.0 GHz	1.0	55
Fe <sub>3</sub> O <sub>4</sub> @graphene/polyetherimide	10 wt%	~14-18	8-12 GHz	2.5	56
Graphene/PMMA	5 wt%	~13-19	8.2-12.4 GHz	2.4	16
Graphene/epoxy	15 wt%	~21	8.2-12.4 GHz	NM*	57
Graphene/PVDF	7 wt%	~21 ~28	1-8 GHz 8-12 GHz	NM*	58
PPY/EVA	25 wt %	~30	1-300 MHz	3.2	59
PPY/PE	14 wt%	~35-55	10 kHz-1 GHz	0.1	60
PPY/PU	25 wt%	~15-25	10 kHz-1 GHz	0.5	60
P3OT/PVC	20 wt%	~47	100 kHz-1 GHz	3.0	61
P3OT/PS	20 wt%	~43	100 kHz-1 GHz	3.0	61
P3OT/EVA	20 wt%	~50	100 kHz-1 GHz	3.0	61
PANI/Polyacrylate	65 wt%	~30-79	14 kHz-1 GHz	0.075	62
PANI/PVC	30 wt%	~70	1 MHz-3 GHz	3.2	11
PANI-DBSA/epoxy	38 wt%	~30-60	100 MHz-1 GHz	1.3	63
PANI/PU	10 wt%	~10-27	8.2-12.4 GHz	1.9	13
PANI/SAN	40 wt%	~50-70	50 MHz-12.4 GHz	0.615	64
PANICN/EVA	15 wt%	~40-80	8 GHz	2.0	32
PANI-MWCNT/PS	7 vol %	~23	8.2-12.4 GHz	1.0	14
PANI-MWCNT/PS	30 wt %	~46	12.4-18.0 GHz	2.0	44

\*NM : Not Mentioned

(MWCNTs)) have emerged as promising filler for making polymer composites, due outstanding properties such as metallic electrical conductivity, excellent corrosion resistance and low density along with ultra high strength /modulus and thermal conductivity<sup>2,5,9,14,29,36,38,48,74-82</sup>. In particular, higher intrinsic conductivity ( $10^4$ - $10^6$  S/cm) and aspect ratio (length/diameter ratio) of CNTs (100-5000) compared to other carbon based fillers (e.g., carbon black, graphite, carbon fiber), permit the realization of

conductivity (in nanocomposites) at much lower loadings (very low percolation threshold)<sup>2,74-77,79</sup>. Accordingly, the formation of continuous networks of CNTs within matrix also leads to improvement in electrical and mechanical properties alongwith superior EM response at the same loading level<sup>9,10,12,20,25,27,36,44,47-49,51-53,83</sup>. Further, due to low percolation threshold of CNTs and comparatively less loading levels required for EMI, the bulk physical properties of polymer matrix are not disturbed to an

extent to exert any harmful effect on mechanical properties of resultant nanocomposites. Therefore, CNTs have shown definite potential for developing light-weight and mechanically strong EMI shielding materials. In the past, several systematic studies have been reported on the electrical and EMI shielding properties of CNT-polymer composites<sup>2,5,12,14,20,36,39,44,48,49,52-54,78</sup>

Li *et al.*<sup>48</sup> fabricated SWCNT-epoxy composites and demonstrated the effect of wall defects and aspect ratio of SWCNTs on the EMI SE performance in the 10 MHz to 1.5 GHz range. At 15 wt% SWCNT loading, the SE (Fig. 1, left image) touched 49 dB at 10 GHz and 15-20 dB in the 500 MHz to 1.5 GHz range.

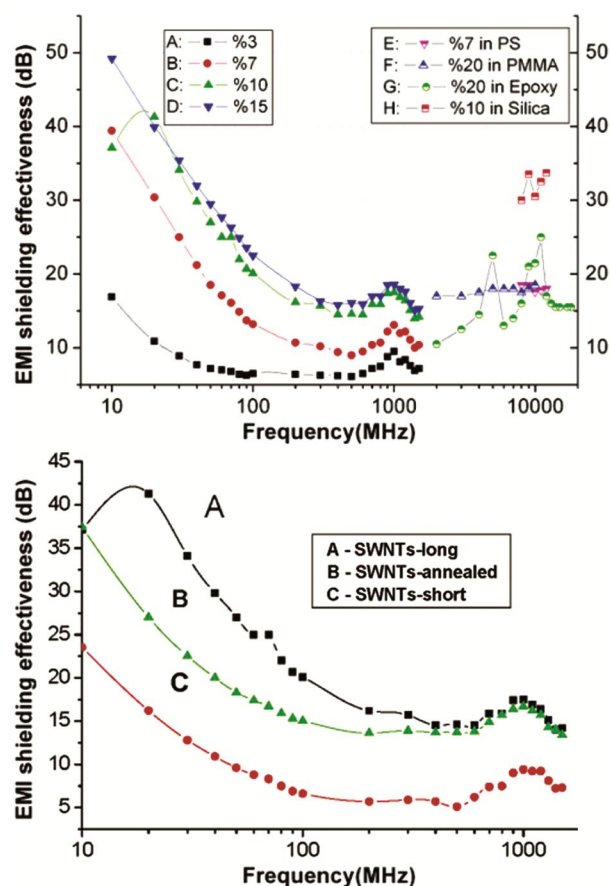


Fig. 1 – EMI shielding effectiveness (plots labeled A-D) for SWCNT-polymer materials (wt % 3-15) studied in this work (10 MHz to 1.5 GHz). Plots labeled E-H are higher frequency data on MWNT-based material presented for comparison: E, MWNTs in PS; F, MWNTs in PMMA; G, MWNTs in epoxy resin and the value of the y axis for G is the reflection loss; H, MWNTs in silica. Impact of wall integrity and aspect ratio on the EMI shielding effectiveness of the composites containing 10 wt % SWCNTs. Reproduced from reference<sup>48</sup> Copyright (2006) American Chemical Society.

It was observed that composites based on SWCNTs-long (having higher SWCNT bundle aspect ratios) display higher conductivities and better EMI shielding performances (Fig. 1, right image) under same loading compared to SWCNT-short composites. It has also been demonstrated that high-temperature annealing of SWNTs in inert gas or vacuum can remove wall defects leading to improved EMI SE value compared to unannealed CNT (SWCNT-short) based composites.

Huang and coworkers<sup>25</sup> have evaluated the EMI shielding performance (in the 8.2-12.4 GHz frequency range) of the epoxy composites based on three different types of SWCNTs (short, long and annealed). It was observed that long-SWCNT-polymer composites (15 wt % loading) possess high real permittivity (polarization,  $\epsilon'$ ) as well as imaginary permittivity (adsorption or electric loss,  $\epsilon''$ ), indicating that such composites could be used as electromagnetic wave absorbers, e.g., for cell phone electronic protection<sup>48</sup>. The complex permittivity spectra of the composites containing 0.01 – 15% of long-SWCNTs Fig. 2(a and b) shows that the real ( $\epsilon'$ ) and imaginary ( $\epsilon''$ ) permittivity increase dramatically as the concentration of the SWCNTs increases from 0.01 to 15 wt%. The highest values of the real and imaginary permittivity parts for the composite with 15% SWCNT loading reach 67 and 76, respectively.

It was also found that composites based on long SWCNTs display better shielding performance Fig. 2(c and d) compared to short-SWCNT composites, with absolute values of 17-18 dB and 23-30 dB, respectively.

The direct effect of filler aspect ratio, loading level and sample thickness on experimental SE along-with theoretical studies was shown by Al-Saleh *et al.*<sup>20</sup> taking polypropylene (PP)/MWCNT system. They reported that SE (in 8.2-12.4 GHz frequency range) of composite plates (1.0 mm thick) made up of 7.5 vol% MWCNT/polypropylene (PP) nanocomposite was almost double (-35 dB) than 7.5 vol% carbon-black (CB)/PP composite (-18 dB). The experimental results showed the involvement of absorption and reflection as major shielding and secondary shielding mechanism, respectively. The modeling results demonstrated that multiple-reflection within MWCNT internal surfaces and between MWCNT external surfaces decrease the overall EMI SE. The EMI SE of MWCNT/PP composites increased with increase in MWCNT content and shielding plate thickness.

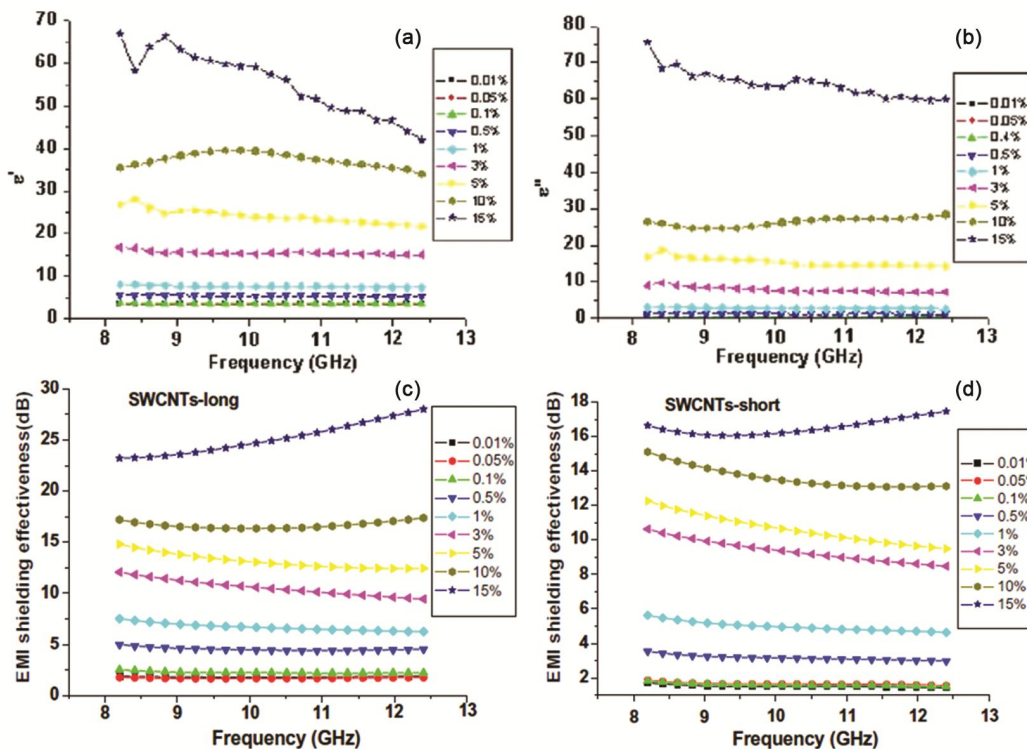


Fig. 2 – Complex permittivity spectra of the composites using ‘long- SWCNTs’ with loading from 0.01 to 15 wt% (a & b). EMI shielding effectiveness for SWCNT (0.01–15 wt%)-epoxy composites containing long and short SWCNTs (c & d). Reproduced from reference<sup>25</sup>, Copyright (2007) Elsevier.

Mahmoodi and coworkers<sup>47,68</sup> investigated the effect of processing method the SE values of 5 wt. % polystyrene (PS)/CNT and polycarbonate(PC)/CNT composites. They found the SE values of ~12 dB and ~17 dB for PS/CNT composites prepared by injection and compression molding techniques respectively, and SE~ -25 dB for injection molded PC/CNT sample. They correlated these results with orientation and dispersion effects of CNTs.

Liu *et al.*<sup>12</sup> achieved only 17 dB attenuation even at 20 wt% MWCNTs loading in polyurethane matrix. Kim *et al.*<sup>52</sup> studied EMI shielding properties of MWCNT/PMMA composites in the range 50 MHz - 13.5 GHz and reported up to 27 dB shielding effectiveness at a high (40 wt%) loading of MWCNT. The contribution of absorption to the total EMI SE was more than that of reflection that was attributed to the presence of iron in the internal cavity of MWCNT.

Singh *et al.*<sup>54</sup> prepared high aspect ratio multi-walled carbon nanotubes (MWCNTs) reinforced low density polyethylene (LDPE) composites with average value of EMI-SE reaches ~23 dB for 10 wt% MWCNT loading. Gupta *et al.*<sup>84</sup> synthesized poly(trimethylene terephthalate) [PTT]/multiwalled

carbon nanotube [MWCNT] with SE of ~23 dB for the composite having 4.76 vol% MWCNT loading. It has also been observed that, as the loading level of the filler increases both electrical conductivity as well as dielectric properties show improvement, leading to proportionate enhancement of absorption and reflection losses (Fig. 3(a)). Several attempts have also been made to enwrap (surface coating involving physical interaction)<sup>9,14,44,78,81</sup> the CNTs with polymeric materials leading to better CNT dispersion along-with improved dielectric properties and enhanced microwave absorption response.

Saini *et al.*<sup>44</sup> loaded (10, 20 and 30 wt. %) polyaniline (PANI) coated multiwall carbon nanotubes (MWCNT) in polystyrene matrix and found that the percolation threshold was only 0.5 wt % and total shielding ( $SE_T$ ) increases (Fig. 3(a)) with increasing MWCNT content as well as sample thickness, reaching a maximum value of 45.7 dB. The reflection loss ( $SE_R$ ) was found to increase slightly from 1.5 to 4.8 dB (Fig. 3(b)) with the increase in weight fraction of PANI-MWCNT that was ascribed to increase in the conductivity. On the other hand, absorption loss ( $SE_A$ ) exhibited rapid enhancement from 9.4 to 19.2 dB with the increased PANI-

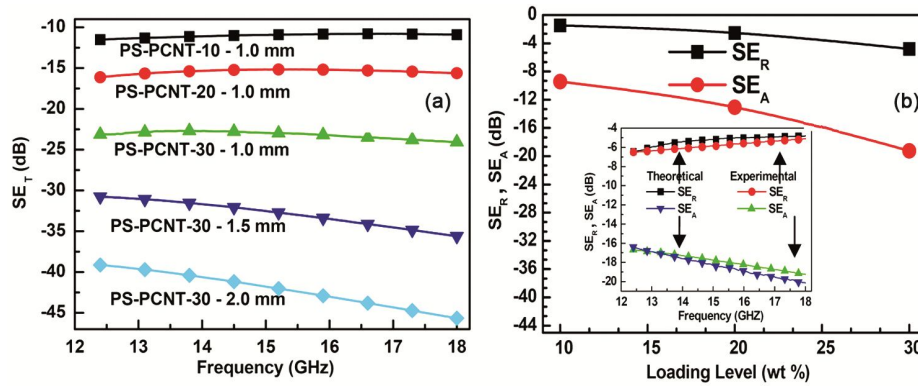


Fig. 3 – (a) Frequency dependence of  $SE_T$  and (b) variation of  $SE_R$  and  $SE_A$  with loading of PANI-MWCNT. Inset shows the theoretical and experimental  $SE_R$  and  $SE_A$  value of the composite (PCNT30) in the 12.4–18.0 GHz frequency band. Reproduced from reference<sup>44</sup>, Copyright (2011) Elsevier.

MWCNT loading. The results confirmed that the observed  $SE_T$  values were dominated by absorption. Hybrid approach where CNT decorated fillers such as carbon fibers/cloth is used as multi-scale conducting reinforcement has also been adopted to fabricate composites with improved electrical, thermal and electromagnetic response (~51 dB for CF-MWCNT/epoxy multiscale composites)<sup>85</sup>. Besides, high CNT content (>50 wt%) yet mechanically strong (tensile strength~2088 MPa, modulus~169 GPa) CNT nanocomposites have also been prepared<sup>86</sup> by adopting a simple mechanical stretching and pre-pegging (pre-resin impregnation) processes on initially randomly dispersed, commercially available sheets of millimeter-long MWNTs that leads to substantial alignment enhancement, good dispersion, and unprecedentedly high electrical conductivity (5500 S/cm). It is important to highlight that different researchers have reported different percolation/conductivity/EMI shielding values even for the same matrix polymer. These observations suggest that SE of CNT filled polymer nanocomposites depends on many factors including fabrication techniques, type of CNT, level of dispersion and nature of host matrix<sup>9</sup>.

Recently, buckypaper (BP) composites (more than 50 wt% loading of nanotubes in BP composite without losing the mechanical properties) have been prepared by resin infiltration technique<sup>87</sup>. Unlike other CNT composites, BP composites can achieve a high concentration of CNTs and high conducting nanotubes networks to further improve EMI shielding effectiveness (SE). Nanocomposite laminates consisting of various proportions of single-walled and multi-walled carbon nanotubes, having different conductivities, and with different stacking structures,

were studied. Single-layer BP composites showed shielding effectiveness (SE) of 20–60 dB, depending on the BP conductivity within a 2–18 GHz frequency range. The results were also compared against the predictions from a modified EMI SE model. The predicted trends of SE value and frequency dependence were in consistent with the experimental results, revealing that adjusting the number of BP layers and appropriate arrangement of the BP conducting layers and insulators can increase the EMI SE from 45–100 dB owing to the utilization of the double-shielding effect.

Saini *et al.*<sup>14</sup> have prepared PANI-MWCNTs/PS composites which were fabricated by solution processing route using non-covalently functionalized (PANI coated) MWCNTs. These composites exhibit an extremely low percolation threshold (0.12 vol.% MWCNT) along with micro porosity and are found to have potential applications in the areas of electromagnetic interference (EMI) shielding and electrostatic dissipation (ESD) with an ESD time of 0.78 s and shielding effectiveness of 23.3 dB (>99 % attenuation). The EMI shielding (Fig. 4(a)) was found to be dominated by absorption (18.7 dB) with a nominal contribution from reflection (4.6 dB) that can explained in terms of multiple internal reflection phenomenon (Fig. 4(b)) driven by high conductivity and the porous structure.

Yang *et al.*<sup>5</sup> studied the EMI shielding behavior of MWCNT/PS foamed nanocomposites and achieved SE of ~ 20 dB at 7 wt % MWCNT loading. The EMI SE measurements indicated that such foam composites with specific SE be 33.1 dB.cm<sup>3</sup>/g (which is much higher than that of typical metals (compared to 10 dB.cm<sup>3</sup>/g for solid copper)<sup>2,66</sup> can be used as very effective, lightweight shielding materials.

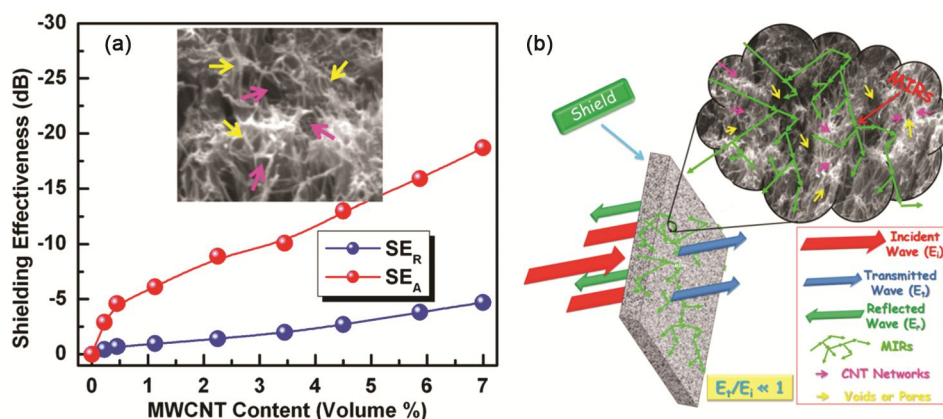


Fig. 4 – (a) Variation of reflection ( $SE_R$ ) and absorption ( $SE_A$ ) losses with MWCNT loading and magnified SEM image (inset) showing dispersed CNTs and voids and (b) schematic representation of radiation shield interaction and involved multiple internal reflection (MIR) phenomenon. Reproduced from reference<sup>14</sup>, Copyright (2013) Springer.

### 3.2 Graphene

Recently, nanoscale materials based on single/multi-layered 2-D graphene sheets have attracted much attention recently due to unusual properties<sup>2,88-91</sup>. Graphene is known as thinnest (one carbon atom thick) yet strongest material (on the basis of specific strength) compared to other carbon allotropes (graphite, carbon fibers, fullerenes, CNTs etc.) or conventional metals. In addition, graphene also possesses exceptional electrical and thermal properties making it promising candidate for electronics and EMI shielding applications<sup>2,9,16,55,88,89,91,92</sup>. Recently with the identification of methods for handling graphene, several attempts have also been made to utilize the fascinating and promising properties of these individual graphitic sheets by formation of graphene based nanocomposites<sup>2,9,16,57,58,88-91,93</sup>, particularly for electrical and electromagnetic shielding applications<sup>2,9,16,55-58</sup>. Like CNTs, here again it is expected that the use of graphene, with large aspect ratio and high conductivity would provide a high EMI SE.

Liang *et al.*<sup>57</sup> fabricated composites based on graphene sheets by incorporating solution-processable functionalized graphene (SPFG) into an epoxy matrix, and their EMI shielding was studied in (Fig. 5(a)). The composites show a low percolation threshold of 0.52 vol %. EMI shielding effectiveness was tested over a frequency range of 8.2–12.4 GHz (X-band), and 21 dB shielding efficiency was obtained for 15 wt% (8.8 vol.%) loading, indicating that they may be used as lightweight, effective EMI shielding materials.

Eswaraiah *et al.*<sup>58</sup> have prepared functionalized graphene (f-G)- polyvinylidene fluoride (PVDF) nanocomposites investigated their and electrical conductivity and electromagnetic interference (EMI) shielding efficiency as a function of mass fractions of f-G. An EMI shielding effectiveness of ~20 dB (Fig. 5(b)) was obtained in X-band (8–12 GHz) region and ~18 dB in broadband (1–8 GHz) region for 5 wt. % composite. The authors reported the reflectivity (R), transmissivity (T), and absorptivity (A) are 0.78, 0.01, and 0.21, respectively, for the PVDF composite containing 5 wt.% of f-G and the reflectivity increases from 10 to 80% with the increase in mass fraction of f-G from 1 to 5 wt.-%. It was also concluded that such f-G/PVDF composites were more reflective and less absorptive to electromagnetic radiation in both X-band and broadband frequencies, i.e., the primary EMI shielding mechanism of such composites was reflection rather than absorption.

Zhang *et al.*<sup>16</sup> prepared graphene-PMMA nanocomposites with much lower percolation (0.52 vol. % graphene) compared to that of the bulk nanocomposites. These nanocomposites (1.8 vol % loading) not only exhibited a high conductivity of 3.11 S/m, but also a good EMI shielding efficiency of 13 to 19 dB at the frequencies range of 8 to 12 GHz. The above results correspond to specific EMI shielding effectiveness (EMI shielding efficiency divided by density) of 17-25 dB cm<sup>3</sup>/g.

Ling and coworkers<sup>94</sup> have prepared polyetherimide (PEI)/graphene nanocomposites foams with specific electromagnetic interference (EMI) shielding effectiveness from 17 to 44 dB.cm<sup>3</sup>/g (Fig. 5(c)), much better compared to other graphene based

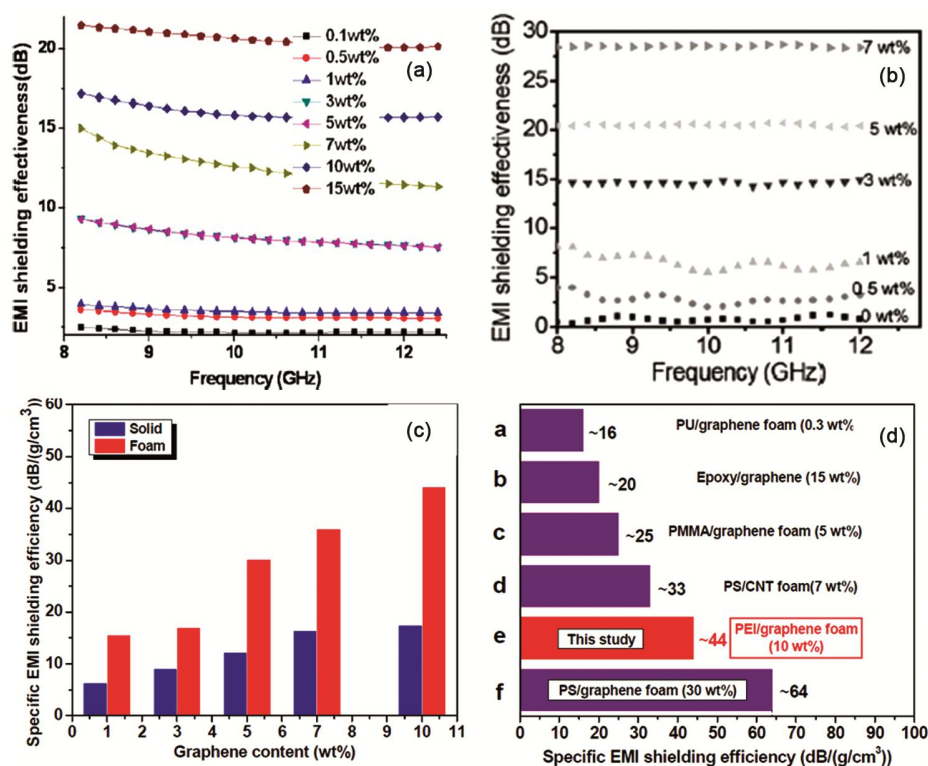


Fig. 5 – (a) EMI SE of graphene/epoxy composites with various SPFG loadings as a function of frequency in the X-band. The graphene/epoxy composites exhibited SE~21 dB in the X-band for a 15 wt% loading. Reproduced from reference<sup>57</sup>, Copyright (2009) Elsevier, (b) EMI SE for f-G-PVDF composites in the X-band range, 8–12 GHz. Reproduced from reference<sup>58</sup>, Copyright (2009) Elsevier, (c) The specific EMI shielding efficiency of PEI/graphene nanocomposites and microcellular foams at 9.6 GHz and (d) the comparative of specific EMI shielding efficiency of our data with other reported results. Reproduced from reference<sup>94</sup>, Copyright (2013) American Chemical Society.

systems (Fig. 5(d)). The detailed investigation of shielding mechanism of graphene based foamed composites revealed that increase of graphene content leads to the improvement of both reflection as well as absorption loss, e.g., PMMA/graphene nanocomposite foam with 1.8 vol % graphene sheets display  $SE_R$ ,  $SE_A$  and  $SE_T$  values of 1, 18, and 19 dB, respectively (Fig. 6(a and b)), which revealed the relative dominance of absorption<sup>16</sup>. However, it is important to point out that reflection is found to be the major contributor to EMI shielding by CNF- and CNT-filled polystyrene foams as well as CNT-filled epoxy and polyurethane nanocomposites<sup>3,5,9,12,25,62</sup>.

### 3.3 Intrinsically conducting polymers

Intrinsically conducting polymers (ICPs) are another extremely important alternative for electrical and EMI shielding applications<sup>2,8–10,13,19,30,34,41,60,65–67,73,95–97</sup>. These materials combine moderate conductivity, good compatibility and ease of processability (as compared with carbons) with low density (~1.1–1.3 g/cm<sup>3</sup> compared to metals, e.g., 8.9

g/cm<sup>3</sup> for copper) and corrosion resistance (compared to metals)<sup>4,96,98–106</sup>. The intrinsic conductivity of conjugated polymers in the field of microwave absorption (100 MHz to 20 GHz) makes them viable materials. In particular, dependence of their conductivity on frequency, many ideas have been attempted to adapt these phenomenon to microwave applications<sup>2,9,10,30,32,96,97,107,108</sup>. The unique properties like tunable conductivity (between insulating and metallic limits), adjustable permittivity/permeability via synthetic means, low density, non-corrosiveness, nominal cost, facile processing (melt or solution), and controllable electromagnetic attributes, further strengthen their candidature as futuristic shielding materials<sup>4</sup>.

The first systematic study of EMI shielding behavior of conducting polymer (PANI) based thermoplastic blends was reported by Colaneri and coworkers<sup>11,65</sup>.

The EMI SE values of these highly conducting blends (~20 S/cm) were measured over a frequency range of 1 MHz to 3 GHz (Fig. 7(a)) and also



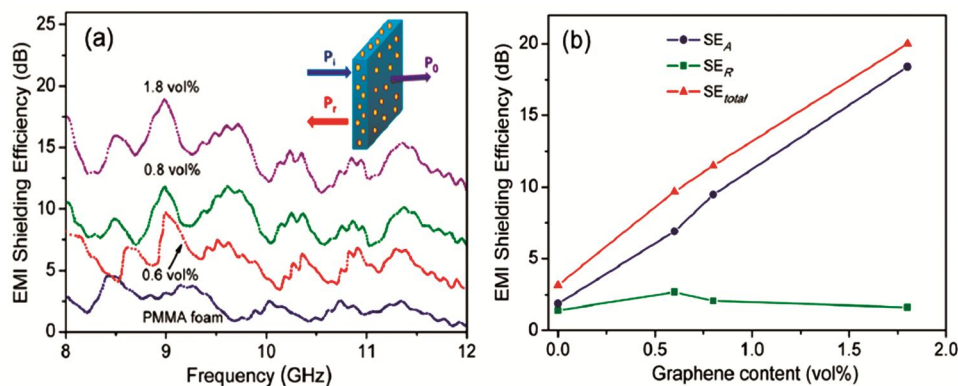


Fig. 6 – (a) EMI shielding efficiency of graphene-PMMA nanocomposite microcellular foams with different contents of graphene sheets and (b) the comparison of  $SE_{total}$ , microwave absorption ( $SE_A$ ), and microwave reflection ( $SE_R$ ) at 9 GHz. Reproduced from reference<sup>16</sup>, Copyright (2011) American Chemical Society.

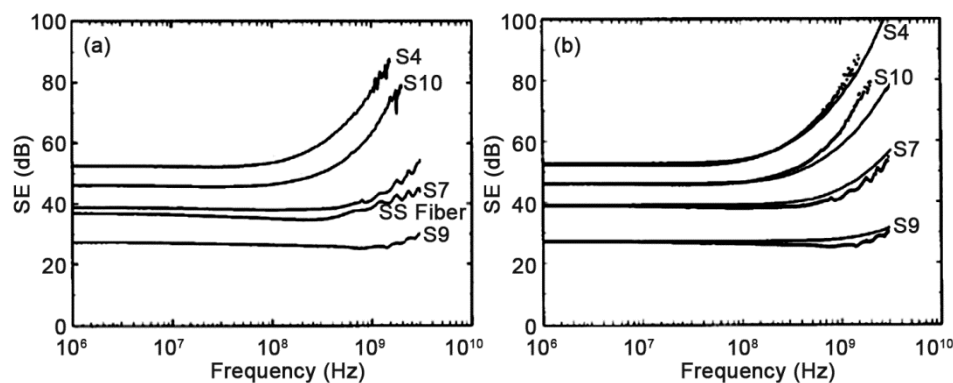


Fig. 7 – (a) Measured far field shielding effectiveness of PVC-ICP blend samples (S4, S10, S7 and S9) of different conductivities (S4: 7.45 S/cm, S10: 3.74 S/cm, S7: 0.98 S/cm and S9: 0.18 S/cm) compared to stainless steel (SS) filled ABS sample and (b) measured far-field shielding results (dots) are compared with the predictions of above samples (solid lines) Reproduced from reference<sup>11</sup>, Copyright (2011) IEEE.

calculated theoretically (Fig. 7(b)) under both near and far field regimes. The far field SE of 70 dB was obtained for the melt blend of polyaniline (30 wt. %) with polyvinyl chloride or nylon which agreed well with the theoretical calculations as per expressions derived by authors.

Later on Taka *et al.*<sup>61</sup> prepared poly(3-octyl thiophene) composites by mixing chemically synthesized poly(3-octyl thiophene) PS, PVC, and EVA in the melt state using a Brabender mixer and tested for EMI shielding at frequency range from 100 kHz to 1 GHz. EMI SE of the composites (3 mm thick) increased with the polymer loadings and 45 dB (from 100 kHz to 10 MHz) was achieved with a polymer loading of 20% in the PVC matrix, though it is still lower than that of a nickel coated sample (80 dB). Pomposo *et al.*<sup>59</sup> have prepared PPY based conducting hot melt adhesives by melt mixing appropriate amounts of ethylene-co-vinyl acetate

(EVA) copolymer and PPY, Far field SE values of 22, and 30 dB were determined (in the 1 to 300 MHz frequency range) for PPY loadings of 15 and 25%, respectively.

Wessling<sup>34</sup> prepared highly conductive blends of PANI with PVC, PMMA or polyester at Ormecon Chemie, with conductivities of 20 S/cm and in some cases even up to 100 S/cm. These blends exhibited EMI SE of 40 to 75 dB for both near and far field conditions. However, mechanical properties were not encouraging and demanded considerable improvement.

Wojkiewicz *et al.*<sup>35</sup> have synthesized PANI/styrene-acrylonitrile (SAN) composites and measured their EMI SE in the frequency ranges of 50 MHz to 1 GHz, 8.2–12.4 GHz and 30–110 GHz. The SAN composite with PANI (40% loading) exhibited SE of 50-70 dB (50 MHz to 1 GHz) and 60-70 dB (8.2–12.4 GHz). Joo & Epstein<sup>52</sup> have demonstrated that electrical conductivity is not the sole scientific

criteria for exhibiting high shielding effectiveness and good attenuations were also extended by moderate conductors with good dielectric properties. It was demonstrated that shielding effectiveness increases with absolute value of complex dielectric permittivity.

It is important to note that, for a given ICP–matrix system, the electrical properties of the resultant composites critically depend on loading level of filler and the involved processing technique<sup>4,9,13,44,59,63,64,73</sup>. The higher filler content leads to the enhancement of number of conducting links and improvement of inter-particle charge transport (by tunneling or hopping phenomenon) resulting in improvement of electrical conductivity. Similarly, selection of proper processing technique helps in the improvement of dispersion of ICPs particles so that continuous conducting network can be achieved at relatively lower loading level. It is also worth pointing out that incorporation of ICP in polymeric matrices not only leads to establishment and improvement of electrical conductivity but also contribute towards improvement of dielectric properties<sup>2,9,13,18,44,63,109</sup> (Fig. 8(a, b)). Such polarization and related relaxation phenomenon contribute towards energy storage and losses, respectively.

Recently, it has also been shown that well-dispersed ICPs (e.g., PANI nanoparticles within epoxy matrix) not only provide a continuous conducting network but also facilitate better charge delocalization leading to huge negative permittivity (Fig. 8(b)) which is a characteristic signature of left handed materials (LHM)<sup>9,63,109</sup>. Interestingly, though EMI shielding is closely related to electrical conductivity but the factors affecting EMI are more complex because they not only involve conduction (leading to ohmic losses) but also polarization phenomenon (due to presence of polarons/bipolarons, dipoles and filler-matrix interfacial polarization). For example, when PANI-DBSA NPs (filler) were added in the epoxy (matrix)<sup>63</sup>, both the conductivity and dipole density increased due to formation of conductive networks. But any excess addition of PANI-DBSA (i.e., beyond the percolation threshold of 28 wt % PANI-DBSA) did not benefit the electrical conduction, because of NP aggregation. However, it did result in more dipolar and interfacial polarization in the hybrid material. Therefore, 38 wt % PANI-DBSA/epoxy improved the EMI shielding efficiency (Fig. 8(c and d)) to ~30-60 dB (in

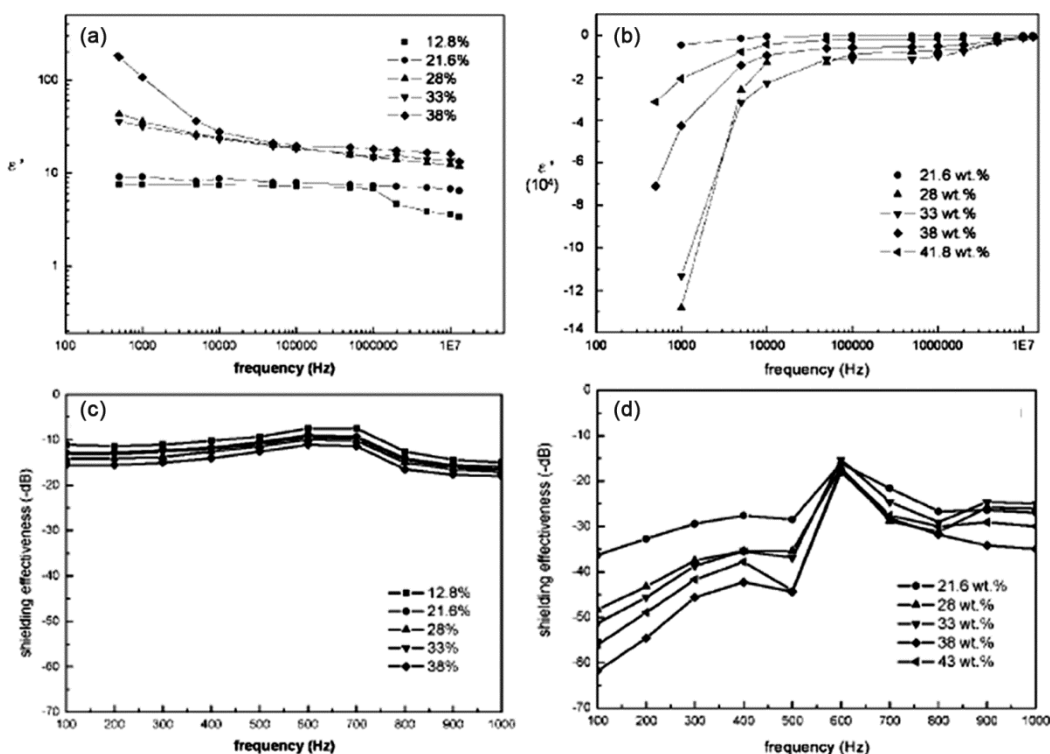


Fig. 8 – Frequency dependence of the dielectric constant ( $\epsilon'$ ) for PANI-DBSA/epoxy hybrids prepared using the (a) blending and (b) absorption transferring processes. EMI shielding effectiveness toward electric fields plotted with respect to frequency (100 MHz-1 GHz) for PANI-DBSA/epoxy hybrids prepared using the (c) blending and (d) absorption-transferring processes. Reproduced from reference<sup>63</sup>, Copyright (2008) American Chemical Society.

100–1000 MHz range) without much enhancement of conductivity.

When ICPs are combined with other conducting fillers, significant reduction in percolation threshold, higher conductivity and better shielding performance is observed as compared to pristine ICPs. This may be attributed to bridging of metallic islands of ICPs (granular metals) as well as better dispersion of ICP coated fillers within various host matrices. For example, PANI coated MWNT epoxy composites display improved microwave absorption response<sup>9,14,44,110,111</sup>. For many applications, e.g., radar absorbers shield should contain electric and/or magnetic dipoles that can interact with the orthogonally pulsating electric and magnetic fields of the incident EM radiation<sup>2,7,9,108,112</sup>. Combination of ICPs with various inorganic fillers with high permittivity or permeability (e.g., ferrites, titanates or other oxides) can give unique combination of properties like moderate electrical conductivity and good dielectric/magnetic properties so that superior shielding performance can be realized. Therefore, numerous attempts have also been made to introduce dielectric or fillers alongwith ICPs to obtain enhanced shielding response arising from balanced

combination of ohmic, dielectric and magnetic losses<sup>4,9,10,17,18,31,66,67,70,110,113–115</sup>. The electric field loss is caused by the dielectric relaxation effect associated with permanent and induced molecular dipoles. As the frequency of incident EM wave increases (especially in the microwave region), dipole present in the system fails to maintain in-phase movement with rapidly pulsating electric vector. Such out-of-phase movement of dipoles leads to molecular friction resulting in energy dissipation in the form of heat. In contrast, magnetic losses are related to permeability of the material and occur due to phenomenon such as hysteresis, eddy-currents, domain wall movement or ferromagnetic resonance. Therefore, microwave absorption is combined effect of dielectric and magnetic losses along with finite conductivity and matching thickness. For example, dielectric PANI/epoxy composites display only dielectric losses compared to hybrid PANI/Fe<sub>3</sub>O<sub>4</sub>/epoxy nanocomposites<sup>116</sup>, which display both dielectric as well magnetic losses (Fig. 9).

It is worth mentioning that due to underlying dielectric and magnetic losses, materials with high permittivity and/or permeability are expected to display good microwave absorption<sup>1,8–10,23,47,56,57,61,66,103</sup>

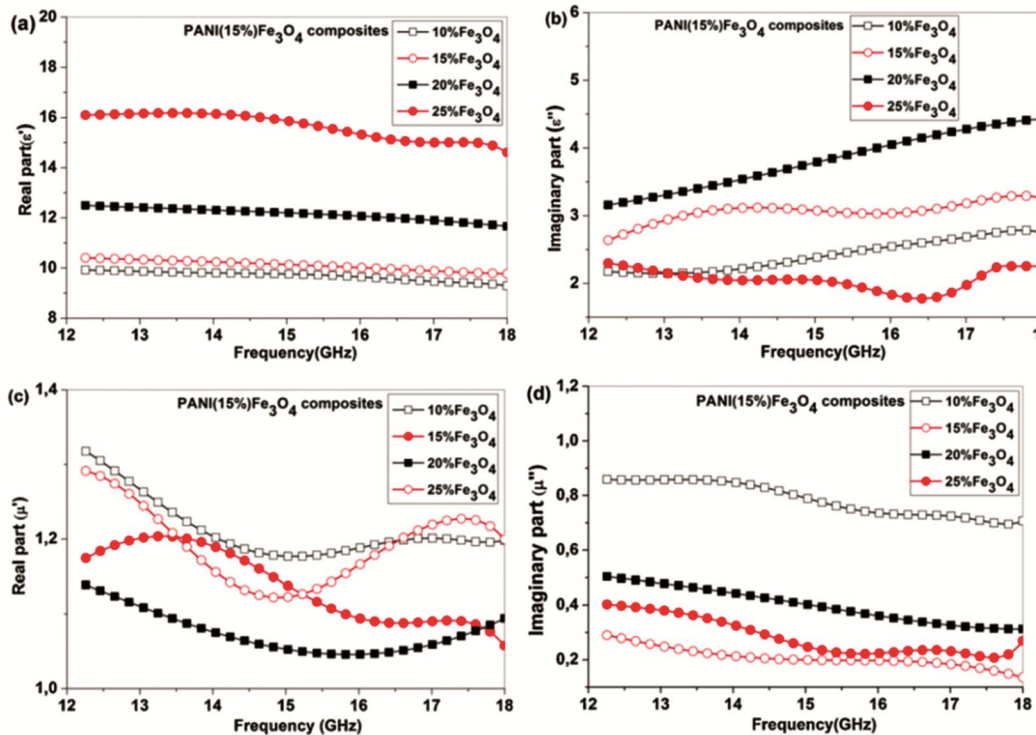


Fig. 9 – The PANI-PTSA (15%)/Fe<sub>3</sub>O<sub>4</sub>/epoxy resin hybrid composites frequency dependence of (a) real part of complex permittivity, (b) imaginary part of complex permittivity, (c) real part of complex permeability and (d) imaginary part of complex permeability. Reproduced from reference<sup>116</sup>, Copyright (2012) Elsevier.

response, e.g., epoxy composite containing 15% of PANI and 10% of  $\text{Fe}_3\text{O}_4$  ( $\epsilon' = 10$ ) gives return loss of -42 dB (at 16.3 GHz) whereas composite of 15% of PANI and 25% of  $\text{Fe}_3\text{O}_4$  ( $\epsilon' = 17$ ) gives return loss of -37.4 dB (at 14.85 GHz). In comparison, a purely dielectric composite with 20% of PANI ( $\epsilon' = 8.5$ ) show a minimum reflection coefficient of only -11 dB (at 18 GHz).

#### 4 Conclusions

It is clear that conducting fillers like ICPs, CNTs and graphene present an attractive solution for realizing efficient EMI shielding materials. However, regardless of their outstanding properties and high aspect ratios, CNTs/graphene based composites have still not been able to touch the theoretically predicted/ultimate limits. In particular, problems involving uniform dispersion, prevention of agglomeration and improved interfacial interaction with host matrices must be addressed to realize their full technical potential for development of advanced nanocomposites for structural and EMI shielding applications. Similarly, despite of their facile processing, ability to accommodate dielectric/magnetic fillers and good compatibility with various matrices, ICPs possess drawbacks like low intrinsic conductivity (compared to metals/carbonaceous materials), high percolation threshold and poor mechanical reinforcing ability, which is a biggest hurdle in their use for making commercially viable EMI shielding materials. Nevertheless, to overcome the limitations of existing materials for realization state-of-the-art EMI shielding materials, complex methodologies are suggested including strategic combination of materials (conducting polymers, carbon based materials and dielectric/magnetic nano-fillers) as well as engineered designs including multilayered structures, multi-scale materials, foamed materials and/or their combination.

#### Acknowledgement

Author is thankful to Director, NPL for encouragement and support for the work. Special thanks to all lab members for their technical assistance and cooperation. Financial assistance by DST via Fast Track Grant for Young Scientists and CSIR by Young Scientist Award Grant are gratefully acknowledged.

#### References

- Ott H W, *Electromagnetic Compatibility Engineering*; John Wiley & Sons, Inc: Hoboken, NJ, USA, (2009)
- Saini P & Arora M, In *New Polymers for Special Applications*; De Souza Gomes A, Ed; InTech, (2012) 71.
- Paul C R, *Electromagnetics for engineers: with applications to digital systems and electromagnetic interference*; John Wiley & Sons: Hoboken, NJ, 2004
- Saini P, Arora M, Gupta G, Gupta B K, Singh V N & Choudhary V, *Nanoscale*, 5 (2013) 4330.
- Yang Y, Gupta M C, Dudley K L & Lawrence R W, *Nano Lett*, 5 (2005) 2131.
- Chung D D, *Carbon*, 39 (2001) 279.
- Chung D D L, *J Mater Eng Perform*, 9 (2000) 350.
- Joo J & Epstein A J, *Appl Phys Lett*, 65 (1994) 2278.
- Saini P, In *Thermoset Nanocomposites*; Mittal V, Ed; Wiley-VCH Verlag GMBH & Co KGAA: Weinheim, Germany (2013) 211.
- Saini P, Choudhary V, Singh B P, Mathur R B & Dhawan S K, *Mater Chem Phys*, 113 (2009) 919.
- Colaneri N F & Schacklette L W, *IEEE Trans Instrum Meas*, 41 (1992) 291.
- Liu Z, Bai G, Huang Y, Ma Y, Du F, Li F, Guo T & Chen Y, *Carbon*, 45 (2007) 821.
- Lakshmi K, John H, Mathew K T, Joseph R & George K E, *Acta Mater*, 57 (2009) 371.
- Saini P & Choudhary V, *J Nanopart Res*, 15 (2013) 1.
- Yang Y, Gupta M C, Dudley K L & Lawrence R W, *Adv Mater*, 17 (2005) 1999.
- Zhang H B, Yan Q, Zheng W G, He Z & Yu Z Z, *ACS Appl Mater Interfaces*, 3 (2011) 918.
- Abbas S M, Chatterjee R, Dixit A K, Kumar A V R & Goel T C, *J Appl Phys*, 101 (2007) 074105.
- Abbas S M, Chandra M, Verma A, Chatterjee R & Goel T C, *Compos Part A*, 37 (2006) 2148.
- Chandrasekhar P & Naishadham K, *Synth Met*, 105 (1999) 115.
- Al-Saleh M H & Sundararaj U, *Carbon*, 47 (2009) 1738.
- Chiscan O, Dumitru I, Postolache P, Tura V & Stancu A, *Mater Lett*, 86 (2012) 251.
- Fletcher A, Gupta M C, Dudley K L & Vedeler E, *Compos Sci Technol*, 70 (2010) 953.
- He Y, Gong R, Li X, Wang X & Hu Q, *Europhys Lett*, 77 (2007) 68006.
- He Y, Gong R, Nie Y, He H & Zhao Z, *J Appl Phys*, 98 (2005) 084903
- Huang Y, Li N, Ma Y, Du F, Li F, He X, Lin X, Gao H & Chen Y, *Carbon*, 45 (2007) 1614.
- Joo J & Lee C Y, *J Appl Phys*, 88 (2000) 513.
- Kim Y J, An K J, Suh K S, Choi H D, Kwon J H, Chung Y C, Kim W N, Lee A K, Choi, J I & Yoon H G, *IEEE Trans Electromag Compatibility*, 47 (2005) 872.
- Li B W, Shen Y, Yue Z X & Nan C W, *Appl Phys Lett*, 89 (2006) 132504.
- Ma C C M, Huang Y L, Kuan H C & Chiu Y S, *J Polym Sci A: Polym Chem*, 43 (2005) 345.
- Naishadham K & Chandrasekhar P, *IEEE*, 3(1998) 1353.
- Singh P, Babbar V K, Razdan A, Srivastava S L & Puri R K, *Mater Sci Eng B*, 67 (1999) 132.
- Sudha J D, Sivakala S, Prasanth R, Reena V L & Radhakrishnan Nair P, *Compos Sci Technol*, 69 (2009) 358.
- Thomassin J M, Pagnouille C, Bednarz L, Huynen I, Jerome R & Detrembleur C, *J Mater Chem*, 18 (2008) 792.
- Wessling B, *Synth Met*, 93 (1998) 143.
- Wojkiewicz J L, Fauveaux S & Miane J L, *Synth Met*, 135 (2003)127.

- 36 Yang Y, Gupta M C, Dudley K L & Lawrence R W, *J Nanosci Nanotechnol*, 5 (2005) 927.
- 37 Yang Y, Gupta M C & Dudley K L, *Nanotechnology*, 18 (2007) 345701.
- 38 Yuen S M, Ma C C M, Chuang C Y, Yu K C, Wu S Y, Yang C C & Wei M H, *Compos Sci Technol*, 68 (2008) 963.
- 39 Pande S, Singh B P, Mathur R B, Dhama T L, Saini P & Dhawan S K, *Nanoscale Res Lett*, 4 (2009) 327.
- 40 Saini P, Choudhary V & Dhawan S K, *Polym Adv Technol*, 23 (2012) 343.
- 41 Saini P, Choudhary V, Sood K N & Dhawan S K, *J Appl Polym Sci*, 113 (2009) 3146.
- 42 Schulz R B, Plantz V C & Brush D R, *IEEE Trans Electromag Compatibility*, 30 (1988) 187.
- 43 Hong Y K, Lee C Y, Jeong C K, Lee D E, Kim K & Joo J, *Rev Sci Instrum*, 74 (2003) 1098.
- 44 Saini P, Choudhary V, Singh B P, Mathur R B & Dhawan S K, *Synth Met*, 161 (2011) 1522.
- 45 Nicolson A M & Ross G F, *IEEE Trans Instrum Meas*, 19 (1970) 377.
- 46 Weir W B, *Proc IEEE*, 62 (1974) 33.
- 47 Arjmand M, Mahmoodi M, Gelves G A, Park S & Sundararaj U, *Carbon*, 49 (2011) 3430.
- 48 Li N, Huang Y, Du F, He X, Lin X, Gao H, Ma Y, Li F, Chen Y & Eklund P C, *Nano Lett*, 6 (2006) 1141.
- 49 Zhao D L, Li X & Shen Z M, *J Alloys Compd*, 471 (2009) 457.
- 50 Mehdipour A, Rosca I D, Trueman C W, Sebak A R & Hoa S V, *IEEE Trans Electromag Compatibility*, 54 (2012) 28.
- 51 Zhang C S, Ni Q Q, Fu S Y & Kurashiki K, *Compos Sci Technol*, 67 (2007) 2973.
- 52 Kim H M, Kim K, Lee C Y, Joo J, Cho S J, Yoon H S, Pejaković D A, Yoo J W & Epstein A J, *Appl Phys Lett*, 84 (2004) 589.
- 53 Gupta A & Choudhary V, *Compos Sci Technol*, 71 (2011) 1563.
- 54 Singh B P, Prabha, Saini P, Gupta T, Garg P, Kumar G, Pande I, Pande S, Seth R K, Dhawan S K & Mathur R B, *J Nanopart Res*, 13 (2011) 7065.
- 55 Chen Z, Xu C, Ma C, Ren W & Cheng H M, *Adv Mater*, 25 (2013) 1296.
- 56 Shen, B, Zhai W, Tao M, Ling J & Zheng W, *ACS Appl Mater Interfaces*, 5 (2013) 11383.
- 57 Liang J, Wang Y, Huang Y, Ma Y, Liu Z, Cai J, Zhang C, Gao H & Chen Y, *Carbon*, 47 (2009) 922.
- 58 Eswaraiah V, Sankaranarayanan V & Ramaprabhu S, *Macromol Mater Eng*, 296 (2011) 894.
- 59 Pomposo J, Rodri guez J & Grande H, *Synth Met*, 104 (1999) 107.
- 60 Kathirgamanathan P, *Adv Mater*, 5 (1993) 281.
- 61 Taka T, *Synth Met*, 41 (1991) 1177.
- 62 Jing X, Wang Y & Zhang B, *J Appl Polym Sci*, 98 (2005) 2149.
- 63 Liu C D, Lee S N, Ho C H, Han J L & Hsieh K H, *J Phys Chem C*, 112 (2008) 15956.
- 64 Fauveaux S & Miane J L, *Electromagnetics*, 23 (2003) 617.
- 65 Shacklette L W, Colaneri N F, Kulkarni V G & Wessling B, *J Vinyl Additive Technol*, 14 (1992) 118.
- 66 Saini P, Choudhary V, Vijayan N & Kotnala R K, *J Phys Chem C*, 116 (2012) 13403.
- 67 Wang Y & Jing X, *Polym Adv Technol*, 16 (2005) 344.
- 68 Mahmoodi M, Arjmand M, Sundararaj U & Park S, *Carbon*, 50 (2012) 1455.
- 69 Kaynak A, Håkansson E & Amiet A, *Synth Met*, 159 (2009) 1373.
- 70 Gairola S P, Verma V, Kumar L, Dar M A, Annapoorni S & Kotnala R K, *Synth Met*, 160 (2010) 2315.
- 71 Gangopadhyay R, De A & Ghosh G, *Synth Met*, 123 (2001) 21.
- 72 Kazantseva N E, Bespyatykh Y I, Sapurina I, Stejskal J, Vilčáková J & Sába P, *J Magn Magn Mater*, 301 (2006) 155.
- 73 Lee C Y, Song H G, Jang K S, Oh E J, Epstein A J & Joo J, *Synth Met*, 102 (1999) 1346.
- 74 Ajayan P M, Schadler L S, Giannaris C & Rubio A, *Adv Mater*, 12 (2000) 750.
- 75 Ajayan P M, Stephan O, Colliex C & Trauth D, *Science*, 265 (1994) 1212.
- 76 Baughman R H, *Science*, 297 (2002) 787.
- 77 Breuer O & Sundararaj U, *Polym Compos*, 25 (2004) 630.
- 78 Choudhary V & Gupta A, In *Carbon Nanotubes-Polymer Nanocomposites*; Yellampalli, S, Ed; InTech (2011).
- 79 *Carbon nanomaterials*; Gogotsi, I G and Presser V, Eds; Advanced materials and technologies series, 2<sup>nd</sup> Edn CRC Press: Boca Raton (2014).
- 80 Iijima S, *Nature*, 34 (1991) 56.
- 81 *Polymer nanotube nanocomposites: synthesis, properties, and applications*; Mittal V, Ed; Wiley, Scrivener: Hoboken N J, Salem MA (2010).
- 82 Moniruzzaman M & Winey K I, *Macromol*, 39 (2006) 5194.
- 83 Shi S L & Liang J, *Nanotechnol*, 19 (2008) 255707.
- 84 Gupta A & Choudhary V, *J Mater Sci*, 46 (2011) 6416.
- 85 Singh B P, Choudhary V, Saini P & Mathur R B, *AIP Adv*, (2012) 022151.
- 86 Cheng Q, Bao J, Park J, Liang Z, Zhang C & Wang, B, *Adv Func Mater*, 18 (2009) 3219.
- 87 Park J G, Louis J, Cheng Q, Bao J, Smithyman J, Liang R, Wang B, Zhang C, Brooks J S, Kramer L, Fanchasis P & Dorough D, *Nanotechnol*, 20 (2009) 415702.
- 88 Geim A K, *Science*, 324 (2009) 1530.
- 89 Geim A K & Novoselov K S, *Nat Mater*, 6 (2007) 183.
- 90 Ramanathan T, Abdala A A, Stankovich S, Dikin, Herrera-Alonso M, Piner R D, Adamson D H, Schniepp H C, Chen X, Ruoff R S, Nguyen S T, Aksay I A, Prud'Homme R K & Brinson L C, *Nat Nanotechnol*, 3 (2008) 327.
- 91 Stankovich S, Dikin D A, Dommett G H B, Kohlhaas K M, Zimney E J, Stach E A Piner R D, Nguyen S T & Ruoff R S, *Nature*, 442 (2006) 282.
- 92 Meyer J C, Geim A K, Katsnelson M I, Novoselov K S, Booth T J & Roth S, *Nature*, 446 (2007) 60.
- 93 Tripathi S N, Saini P, Gupta D & Choudhary V, *J Mater Sci*, 48 (2013) 6223.
- 94 Ling J, Zhai W, Feng W, Shen B, Zhang J, Zheng W, *ACS Appl Mater Interfaces*, 5 (2008) 2677.
- 95 Saini P, Jalan R & Dhawan S K, *J Appl Polym Sci*, 08 (2008) 1437.
- 96 Chandrasekhar P, *Conducting polymers, fundamentals and applications: a practical approach*; Kluwer Academic: Boston (1999).
- 97 Olmedo L, Hourquebie P & Jousse F, *Synth Met*, 69 (1995) 205.
- 98 Saini P & Arora M, *J Mater Chem A*, 1 (2013) 8926.
- 99 Saini P & Choudhary V, *J Mater Sci*, 48 (2013) 797.
- 100 Chiang C, Fincher C, Park Y, Heeger A, Shirakawa H, Louis E, Gau S & MacDiarmid A G, *Phys Rev Lett*, 39 (1977) 1098.

- 101 Heeger A J, *Angew Chem Int Ed*, 40 (2001) 2591.
- 102 Shirakawa H, Louis E J, MacDiarmid A G, Chiang C K & Heeger A J, *J Chem Soc Chem Commun*, (1977) 578.
- 103 Chiang J C & MacDiarmid A G, *Synth Met*, 13 (1986) 193.
- 104 Kohlman R, Zibold A, Tanner D, Ihas G, Ishiguro T, Min Y, MacDiarmid A G & Epstein A J, *Phys Rev Lett*, 78 (1997) 3915.
- 105 MacDiarmid A G, *Angew Chem Int Ed*, 40 (2001) 2581.
- 106 MacDiarmid A G & Epstein A J, *MRS Proceedings*, (1993) 328.
- 107 Naishadham K & Kadaba P K, *IEEE Trans Microwave Theory Technol*, 39 (1991) 1158.
- 108 Skotheim T A & Elsenbaumer Reynolds, *Handbook of conducting polymers*, M Dekker, New York (1998).
- 109 Hsieh C H, Lee A H, Liu C D, Han J L, Hsieh K H & Lee S N, *AIP Adv*, 2 (2012) 012127.
- 110 Ting T H, Jau Y N & Yu R P, *Appl Surf Sci*, 258 (2012) 3184.
- 111 Makeiff D A & Huber T, *Synth Met*, 56 (2006) 497.
- 112 Knott E F, *Radar cross section*; The Artech House radar library; 2<sup>nd</sup> Edn; Artech House, Boston (1993).
- 113 Xu P, Han X, Jiang J, Wang X, Li X & Wen A, *J Phys Chem C*, 111 (2007) 12603.
- 114 Yang C C, Gung Y J, Hung W C, Ting T H & Wu K H, *Compos Sci Technol*, 70 (2010) 466.
- 115 Kurlyandskaya G V, Cunanan J, Bhagat S M, Apesteguy J C & Jacobo S E, *J Phys Chem Solids*, 68 (2007) 1527.
- 116 Belaabed B, Wojkiewicz J L, Lamouri S, El Kamchi N & Lasri T, *J Alloys Comp*, 527 (2012) 137.
- 117 Eswaraiah V, Sankaranarayanan V & Ramaprabhu S, *Nanoscale Res Lett*, 6 (2011) 137.